Late Transition Metal Oxo and Imido Complexes. 11.[1] Gold(I) Oxo Complexes

Yi Yang, Visalakshi Ramamoorthy, and Paul R. Sharp*

Department of Chemistry, University of Missouri—Columbia, Columbia, Missouri 65211

Received November 24, 1992

The gold(I) oxo complexes $[(LAu)_3(\mu_3\text{-}O)]BF_4$ (**1**) have been prepared for L = $PMePh_2$, PMe_2Ph, $PEtPh_2$, PPr^iPh_2, $P(p\text{-}ClPh)_3$, $P(o\text{-}tol)_3$, $P(OEt)Ph_2$, and $P(OMe)_3$. Two of these new oxo complexes, as well as a new crystal form of $[(PPh_3Au)_3(\mu_3\text{-}O)]BF_4$, were structurally characterized. Crystals of $[(PMePh_2Au)_3(\mu_3\text{-}O)]BF_4\cdot CH_2Cl_2$ from CH_2Cl_2/ether are monoclinic ($P2_1/c$) with a = 11.395(2) Å, b = 25.901(2) Å, c = 16.024(3) Å, β = 110.615(8)°, and Z = 4. Crystals of $[(PPh_3Au)_3(\mu_3\text{-}O)]BF_4\cdot 1.5CH_2Cl_2$ from CH_2Cl_2/ether are monoclinic ($P2_1/c$) with a = 14.723(3) Å, b = 14.808(3) Å, c = 25.999(3) Å, β = 104.06(3)°, and Z = 4. Crystals of $[(P(o\text{-}tol)_3Au)_3(\mu_3\text{-}O)]BF_4\cdot xC_6H_{14}\cdot 0.5H_2O$ from CH_2Cl_2/hexane are monoclinic ($P2_1/a$) with a = 14.2611(45) Å, b = 27.4668(71) Å, c = 23.0907(81) Å, β = 91.37(2)°, and Z = 4. The PPh_3 and the $PMePh_2$ structures consist of inversion-related edge-bridged $[(LAu)_3O]^+$ dimers held together by Au–Au interactions. The $P(o\text{-tol})_3$ structure consists of isolated $[(LAu)_3O]^+$ units. New oxo complexes are also formed in equilibrium mixtures of $[((PPh_3)Au)_3(\mu_3\text{-}O)]BF_4$ and LAuCl. Oxygen-17 NMR data for **1** show chemical shifts of +19.7 to −36.0 ppm (H_2O reference) with upfield shifts corresponding to increasing basicity of the phosphine, L.

Introduction

Many late transition metals have a remarkable ability to adsorb and dissociatively activate molecular oxygen.[2] The resulting surface oxygen atoms (oxygen adatoms) are important intermediates in many catalytic processes and may be modeled by oxo and the isoelectronic imido complexes. This idea, and an interest in the reactivity of late transition metal–oxygen and –nitrogen bonds, has led us to study the synthesis and reactivity of a number of late transition metal oxo and imido complexes. In addition to work on Rh[3] and Pt,[4] we have been exploring the chemistry of the one known Au complex,[5] $[((Ph_3P)Au)_3(\mu_3\text{-}O)]^+$. We, and others, have found that this complex has a rich chemistry and is a versatile reagent for the synthesis of many novel complexes.[6,7] To expand on this chemistry and to investigate the steric and electronic effects of the phosphine on the oxo complexes and their derivatives we have prepared analogues of $[((Ph_3P)Au)_3(\mu_3\text{-}O)]^+$ with a wide range of phosphine ligands in place of PPh_3. The synthesis and characterization of these complexes are described below.

Results

Syntheses. With slight modifications, one of the original procedures for the synthesis of $[((Ph_3P)Au)_3(\mu_3\text{-}O)]BF_4$ is successful for the synthesis of $[(LAu)_3(\mu_3\text{-}O)]BF_4$ for a large range of L = a phosphine. Thus, treating LAuCl (L = $PMePh_2$, PMe_2Ph, $PEtPh_2$, PPr^iPh_2, $P(o\text{-tol})_3$, $P(OEt)Ph_2$, $P(OMe)_3$) with freshly prepared silver oxide in the presence of $NaBF_4$ gives, following workup, 80–90% yields of $[(LAu)_3(\mu_3\text{-}O)]BF_4$ (eq 1).

$$LAuCl + Ag_2O \rightarrow [(LAu)_3(\mu_3\text{-}O)]BF_4 + AgCl \quad (1)$$

In three cases, L = $P(PhO)_3$, $P(PhO)Ph_2$, and $P(p\text{-}ClPh)_3$, this procedure fails but for one, L = $P(p\text{-}ClPh)_3$, an alternate procedure, again a slight modification of a synthesis for $[\{(Ph_3P)Au\}_3(\mu_3\text{-}O)]BF_4$, is successful (eq 2). This procedure is

$$LAuCl \xrightarrow[(2)\ NaOH]{(1)\ AgBF_4} [(LAu)_3(\mu_3\text{-}O)]BF_4 + AgCl \quad (2)$$

also readily adapted to the synthesis of ^{17}O-labeled **1** simply by the addition of small amounts of $H_2{}^{17}O$ (30%) to the carefully dried reaction solvent.

Data for the oxo complexes are given in Table I. Also included are the pK_a values[8] for the phosphine ligands. The ^{31}P NMR spectra show a singlet for the oxo complexes shifted 5–10 ppm upfield from that of the chloride precursor. Cooling ^{31}P NMR samples of **1** (L = $PPhMe_2$) to −80 °C at 202 MHz leads to significant line broadening (the half-height peak width changes from 15 to 49 Hz) but does not result in the resolution of the single line into the two lines expected from the solid-state structure (see below and ref 5).

The O^{17} NMR chemical shifts for **1** cover a range from +19.7 to −36.0 ppm (H_2O reference) and are sensitive to the nature of the phosphine. With the exception of those for **1** (L = PPh_3), the shifts correlate well with the phosphine basicity and show an upfield shift with increasing pK_a. The correlation is approximately linear (r^2 = 0.96) with a slope of ca. −9 ppm/pK_a.

New oxo complexes are also observed in the reaction of $[(LAu)_3(\mu_3\text{-}O)]BF_4$ with L'AuCl (eq 3). Although not a good

$$[(LAu)_3(\mu_3\text{-}O)]BF_4 + L'AuCl \rightleftharpoons [(L'Au)_3(\mu_3\text{-}O)]BF_4 + LAuCl \quad (3)$$

synthetic procedure since an equilibrium mixture is produced,

(1) Part 10: Ge, Y.-W.; Sharp, P. R. *Inorg. Chem.* **1993**, *32*, 94–100.
(2) Madix, R. J.; Jorgensen, S. W. *Surf. Sci.* **1987**, *183*, 27. Akhter, S.; White, J. M. *Surf. Sci.* **1986**, *167*, 101. Berlowitz, P.; Yang, B. L.; Butt, J. B.; Kung, H. H. *Surf. Sci.* **1986**, *171*, 69. Outka, D. A.; Madix, R. J. *J. Am. Chem. Soc.* **1987**, *109*, 1708. Lueng, L.-W. H.; Weaver, M. J. *J. Am. Chem. Soc.* **1987**, *109*, 5113. Roberts, J. T.; Madix, R. J. *J. Am. Chem. Soc.* **1988**, *110*, 8540. Xu, X.; Friend, C. M. *J. Am. Chem. Soc.* **1990**, *112*, 4571.
(3) Ge, Y.-W.; Peng, F.; Sharp, P. R. *J. Am. Chem. Soc.* **1990**, *112*, 2632–2640. Ge, Y.-W.; Sharp, P. R. *Inorg. Chem.* **1992**, *31*, 379–384.
(4) Li, W.; Barnes, C. L.; Sharp, P. R. *J. Chem. Soc., Chem. Commun.* **1990**, 1634–1636.
(5) Nesmeyanov, A. N.; Perevalova, E. G.; Struchkov, Y. T.; Antipin, M. Y.; Grandberg, K. I.; Dyadchenko, V. P. *J. Organomet. Chem.* **1980**, *201*, 343–349.
(6) (a) Ramamoorthy, V.; Sharp, P. R. *Inorg. Chem.* **1990**, *29*, 3336. (b) Ramamoorthy, V.; Wu, Z.; Yi, Y.; Sharp, P. R. *J. Am. Chem. Soc.* **1992**, *114*, 1526–1527.
(7) Schmidbauer, H.; Weidenhiller, G.; Steigelmann, O. *Angew. Chem., Int. Ed. Engl.* **1991**, *30*, 433–435. Grohmann, A.; Riede, J.; Schmidbaur, H. *J. Chem. Soc., Dalton Trans.* **1991**, *783*–787. Smysolova, E. I.; Perevalova, E. G.; Dyadchenko, V. P.; Grandberg, K. I.; Slovokhotov, H. L.; Struchkov, Y. T. *J. Organomet. Chem.* **1981**, *215*, 269–279.
(8) Rahman, Md. M.; Liu, H. Y.; Prock A.; Giering, W. P. *Organometallics* **1987**, *6*, 650–658.

0020-1669/93/1332-1946$04.00/0

Table I. Characterization Data for $[(LAu)_3(\mu_3\text{-}O)]BF_4$ (**1**)[a]

L	anal.[b]	δ ^{31}P NMR	δ ^{1}H NMR[c]	δ ^{17}O NMR[d]	pK_a[e]
P(*p*-ClPh)$_3$		23.6		13.7 (295)	1.03
P(OMe)$_3$	C: 10.1 (10.0) H: 2.6 (2.4)	106.2	3.84 (d, J_{HP} = 13.6)	2.6 (290)	2.60
PPh$_3$	ref 5	24.0		19.7 (152)	2.73
P(*o*-tol)$_3$	C: 47.1 (46.2) H: 4.0 (3.8)	−1.4	2.38 (s)	−17.8 (290)	3.08
PMePh$_2$		8.2	2.20 (d, J_{HP} = 10.5)		4.57
PEtPh$_2$		24.9	2.51 (dq, J_{HH} = 7.5, J_{HP} = 10.9), 1.23 (dt, J_{HP} = 21.4)		4.9
PMe$_2$Ph		−6.2	1.91 (d, J_{HP} = 10.7)	−36.0 (160)	6.50
PPr^{i}Ph$_2$	C: 39.2 (39.7) H: 3.7 (3.6)	40.4	2.84 (dsept, J_{HH} = 6.8, J_{HP} = 18.9), 1.22 (dd, J_{HP} = 19.8)		
P(OEt)Ph$_2$	C: 36.0 (36.3)	100.6	4.17 (dq, J_{HH} = 7.0, J_{HP} = 9.6), 1.41 (t)		
(·H$_2$O)	H: 3.4 (3.2)	100.6	4.17 (dq, J_{HH} = 7.0, J_{HP} = 9.6), 1.41 (t)		

[a] *J* values in hertz. NMR spectra were recorded in CH_2Cl_2 or CD_2Cl_2. [b] Elemental analysis. Calculated values with determined values in parentheses. [c] Non-phenyl resonances. [d] Values in parentheses are the half-height frequency width for the ^{17}O NMR peaks. [e] From ref 8.

Table II. Crystallographic and Data Collection Parameters for $[(LAu)_3(\mu_3\text{-}O)]BF_4$

	L = PMePh$_2$	L = PPh$_3$	L = P(*o*-tol)$_3$
formula	$C_{39}H_{37}Au_3BF_4OP_3{\cdot}CH_2Cl_2$	$C_{54}H_{45}Au_3BF_4OP_3{\cdot}1.5CH_2Cl_2$	$C_{63}H_{63}Au_3BF_4OP_3{\cdot}xC_6H_{14}{\cdot}0.5H_2O$
fw	1377.27	1607.99	1606.83[d]
space group	$P2_1/c$ (No. 14)	$P2_1/c$ (No. 14)	$P2_1/a$ (No. 14)
T, °C	22	22	22
λ, Å	0.710 69	0.710 69	1.5406
a, Å	11.395(2)	14.723(3)	14.2611(45)
b, Å	25.901(2)	14.808(3)	27.4668(71)
c, Å	16.024(3)	25.999(3)	23.0907(81)
β, deg	110.615(8)	104.06(3)	91.37(2)
V, Å^3	4426.5(12)	5498.3(17)	9042(5)
Z	4	4	4
d_{calc}, g cm^{-3}	2.07	1.94	1.18[d]
μ, mm^{-1}	10.2	10.9	10.2[d]
transm range, %	83.7–99.8	*c*	56.7–99.7
$R(F_o)$[a]	0.045	0.037	0.065
$R_w(F_o)$[b]	0.058	0.049	0.103

[a] $R(F_o) = \sum||F_o| - |F_c||/\sum|F_o|$. [b] $R_w(F_o) = [\sum w(|F_o| - |F_c|)^2/\sum wF_o^2]^{1/2}$. [c] Absorption range was less than 3%. A correction was not applied. [d] Assumes no solvent of crystallization.

this is a good method for evaluating the stability of the oxo complexes and for determining their ^{31}P NMR chemical shifts prior to synthetic attempts by the methods shown above (eqs 1 and 2). An interesting feature of the equilibrium systems is that only two ^{31}P NMR peaks are observed for the oxo complexes down to −80 °C. In principle, four different oxo complexes, $[(LAu)_3(\mu_3\text{-}O)]BF_4$, $[(LAu)_2(L'Au)(\mu_3\text{-}O)]BF_4$, $[(LAu)(LAu)_2(\mu_3\text{-}O)]BF_4$, and $[(L'Au)_3(\mu_3\text{-}O)]BF_4$, should be present, representing all possible combinations of the ligands L and L'. The observation of only two signals suggests rapid exchange and/or accidently coincident chemical shifts. In order to investigate this further, we studied the exchange reaction of the imido complex[6a] $[(LAu)_3(\mu_3\text{-}NR)]BF_4$ (**2**) (R = *t*-Bu, L = PPh_2Me) with L'AuCl (L' = PPr^{i}Ph$_2$) and the interaction of the imido complexes $[(LAu)_3(\mu_3\text{-}NR)]BF_4$ and $[(L'Au)_3(\mu_3\text{-}NR)]BF_4$ (**2**) (R = *t*-Bu, L = PPh_3, L' = PPh_2Me). For the imido/imido mixture at 25 °C, only two imido peaks are observed in the ^{31}P NMR spectra. However, when the sample is cooled to −80 °C, the two peaks are resolved into a total of five peaks. (A total of six peaks would be expected for the four possible imido complexes if there was no overlap.) For the imido/Cl mixture with the bulkier phosphine, six peaks are observed even at 25 °C.

Structures. An interesting feature of the reported solid-state structure of $[((Ph_3P)Au)_3(\mu_3\text{-}O)]BF_4$ is the presence of both intra- and intercation Au–Au bonds.[5] The presence of the intercation Au–Au bonds leads to an ion dimer structure where the two pyramidal $(LAu)_3O^+$ units are edge-bridged through two Au atoms and are related by an inversion center (see Figure 1b). The availability of the range of oxo complexes prepared here gives us the opportunity to probe the effect of the phosphine ligands on these and other interactions in the oxo cations. The crystal structures of three Au oxo complexes, one a new crystal form of $[((Ph_3P)Au)_3(\mu_3\text{-}O)]BF_4$, were determined.

A summary of crystallographic and data collection parameters for the structures is given in Table II. Selected crystallographic coordinates are given in Table III. Selected interatomic distances and angles are given in Table IV, and ORTEP drawings are shown in Figure 1. The greatest change in the solid-state structures is the disruption of the edge-bridged cation dimer on going from the smaller phosphines, PPh_3 and $PMePh_2$, to the larger phosphine, P(*o*-tol)$_3$. The reason for this is apparent from the ORTEP diagram of the P(*o*-tol)$_3$ structure (Figure 1c) which shows that the *o*-methyl groups of the phosphine are positioned so as to block dimer formation. That dimer formation is subject to steric stress is evidenced by an increased interion Au–Au distance on going from the $PMePh_2$ (3.062(1) Å) to the PPh_3 (3.115(1) Å) structure. Crowding in the dimer is also shown by the angle of the interion gold–gold interaction. In sterically open structures, the Au–Au interactions are orthogonal to the linear two-coordinate axis of Au(I).[9] In the $PMePh_2$ oxo complex, the angles are close to the ideal of 90° (90.3(1) and 92.3(3)°) but are considerably further from this in the more crowded PPh_3 complex (104.44(9) and 79.0(2)°). Another way of seeing this is in the angle between the four-membered plane formed by Au1, Au2, Au1', and Au2' and the three-membered plane of Au1, Au2, and Au3. In the $PMePh_2$ complex, this angle is 49° and is set by close contact between the oxo oxygen and the methyl group of P1 and R4 of P2 on the inversion-related cation (*d*(C1–O) = 3.44 and *d*(C46–O) = 3.43 Å). A larger value of 57° is

(9) (a) Jones, P. G. *Gold Bull.* **1981**, *14*, 102, 159; **1983**, *16*, 114; **1986**, *19*, 46. (b) Schmidbaur, H. *Gold Bull.* **1990**, *23*, 11.

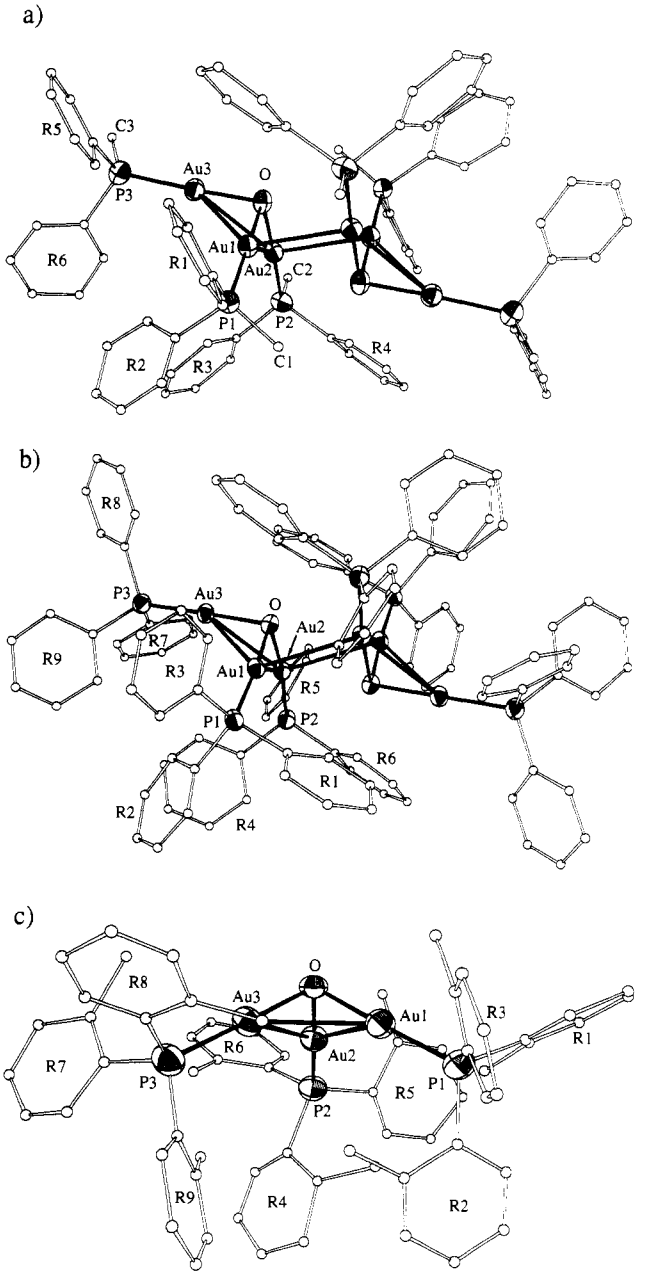

Figure 1. ORTEP drawings of **1** (50% probability ellipsoids): (a) L = PPh_2Me (the two cations are related by an inversion center); (b) L = PPh_3 (the two cations are related by an inversion center); (c) L = P(*o*-tol)$_3$.

found in the PPh_3 structure and results from the greater steric demand of PPh_3: the ion tips to get the phenyl rings (R1 and R6) of P1 and P2 away from the oxo group and maintain reasonable distances (d(C16–O) = 3.39 and d(C66–O) = 3.41 Å). This analysis also clearly shows why the analogous imido complexes[6a] do not have the edge-bridged structure: the replacement of the oxo ligand with an NR group would leave no room for the phosphine ligands.

Although differing in oligomerization, other features of the three structures involving the $(LAu)_3O$ unit are very similar. Notably, the average Au–O distances do not vary at all and are equal at 2.05 Å. What does change with the size of the phosphines is the average intraion Au–Au distances (3.054, 3.069, and 3.086 Å) and the average Au–O–Au angles (96.2, 97.0, and 97.6°). This can be described as an expansion of the structure (or a flattening of the pyramid) to accommodate the increasing steric demand of the phosphine ligand. The effect, though small, may also be observed in the decreasing distance of the oxo oxygen atom to the Au_3 plane ($PMePh_2$, 1.05(1) Å; PPh_3, 1.02(1) Å; P(*o*-tol)$_3$, 1.01(1) Å).

Table III. Selected Positional Parameters for $[(LAu)_3(\mu_3\text{-}O)]BF_4$ (**1**)

	x	y	z	B, Å^2
		L = $PMePh_2$		
Au1	0.98753(8)	0.47965(3)	0.11364(5)	3.58(4)
Au2	1.02804(8)	0.58711(3)	0.04760(5)	3.59(4)
Au3	0.82640(8)	0.56728(3)	0.13216(6)	3.90(4)
P1	1.1108(5)	0.42138(22)	0.2045(4)	3.7(3)
P2	1.1816(5)	0.64325(23)	0.0653(4)	4.1(3)
P3	0.7567(6)	0.59275(24)	0.2384(4)	4.5(3)
O	0.8813(12)	0.5373(5)	0.0340(8)	3.7(7)
		L = PPh_3		
Au1	0.14705(3)	0.52829(3)	0.040015(20)	2.816(25)
Au2	0.04383(4)	0.37171(3)	–0.030641(21)	2.90(3)
Au3	0.19373(4)	0.46374(3)	–0.066493(21)	3.08(3)
P1	0.22612(24)	0.55147(23)	0.12355(14)	3.02(17)
P2	0.01840(25)	0.22549(22)	–0.02143(15)	3.42(19)
P3	0.3060(3)	0.40865(24)	–0.10162(15)	3.53(18)
O	0.0825(5)	0.5044(5)	–0.0372(3)	2.5(4)
		L = P(*o*-tol)$_3$		
Au1	0.06107(6)	0.37737(3)	0.31671(3)	4.79(4)
Au2	–0.04063(5)	0.29295(3)	0.25352(3)	4.36(4)
Au3	0.05556(6)	0.37419(3)	0.18338(3)	4.86(4)
P1	0.0381(4)	0.42942(20)	0.38869(23)	5.6(3)
P2	–0.1761(3)	0.25167(19)	0.25497(21)	4.9(3)
P3	0.0280(4)	0.42445(21)	0.10856(24)	5.7(3)
O	0.0842(7)	0.3278(4)	0.2506(4)	4.2(5)

Table IV. Selected Distances (Å) and Angles (deg) for $[(LAu)_3(\mu_3\text{-}O)]BF_4$ (**1**)

	L		
	$PMePh_2$	PPh_3	P (*o*-tol)$_3$
Au1–Au2	3.0698(12)	3.1151(9)	3.0834(13)
Au1–Au3	2.9992(12)	3.1589(9)	3.0790(16)
Au2–Au3	3.0936(13)	2.9320(9)	3.0968(13)
Au1–Au2a	3.0616(12)	3.1332(9)	
Au1–P1	2.221(6)	2.227(4)	2.223(5)
Au2–P2	2.215(6)	2.220(3)	2.240(5)
Au3–P3	2.217(6)	2.229(4)	2.239(5)
Au1–O	2.058(12)	2.033(7)	2.078(11)
Au2–O	2.061(13)	2.064(7)	2.023(11)
Au3–O	2.039(12)	2.057(7)	2.042(10)
Au2–Au1–Au3	61.28(3)	55.715(19)	60.34(3)
Au1–Au2–Au3	58.24(3)	62.900(21)	59.76(3)
Au1–Au3–Au2	60.48(3)	61.384(25)	59.90(3)
Au2–Au1–Au2a	101.08(3)	90.35(3)	
Au2a–Au1–Au3	130.94(4)	117.19(3)	
Au1–Au2–Au1a	78.92(3)	89.65(3)	
Au1a–Au2–Au3	116.40(4)	119.068(25)	
Au2–Au1–P1	134.83(15)	138.95(9)	139.60(16)
Au3–Au1–P1	135.84(14)	136.71(9)	139.93(15)
Au1–Au2–P2	139.37(15)	137.16(10)	140.30(13)
Au3–Au2–P2	136.72(16)	130.33(9)	139.93(13)
Au1–Au3–P3	134.29(16)	144.20(10)	138.94(16)
Au2–Au3–P3	143.99(17)	130.60(10)	140.90(15)
Au2a–Au1–P1	90.29(14)	104.44(9)	
Au1a–Au2–P2	106.68(16)	107.32(9)	
Au2–Au1–O	41.8(4)	40.88(20)	40.6(3)
Au3–Au1–O	42.7(3)	39.71(21)	41.2(3)
Au1–Au2–O	41.8(3)	40.15(21)	41.9(3)
Au3–Au2–O	40.8(3)	44.54(21)	40.6(3)
Au1–Au3–O	43.2(3)	39.17(21)	42.1(3)
Au2–Au3–O	41.3(4)	44.74(19)	40.2(3)
Au2a–Au1–O	92.3(3)	79.05(21)	
Au1a–Au2–O	75.8(3)	78.69(21)	
P1–Au1–O	176.2(4)	176.41(23)	178.8(3)
P2–Au2–O	177.3(4)	173.90(23)	177.6(3)
P3–Au3–O	174.4(4)	174.60(22)	178.4(3)
Au1–O–Au2	96.4(5)	99.0(3)	97.5(4)
Au1–O–Au3	94.1(5)	101.1(3)	96.7(5)
Au2–O–Au3	98.0(5)	90.7(3)	99.3(4)

Discussion

The flexibility of the syntheses shown in eqs 1 and 2 is remarkable. The phosphine ligands of **1** span almost the full range of steric and electronic properties available and testify to the high stability of the $(LAu)_3O^+$ cation. The ability to

Scheme I

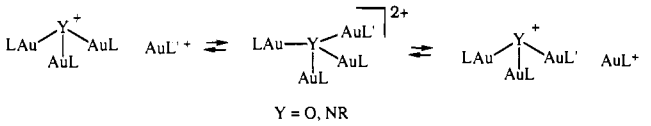

accommodate a wide steric range of phosphines can be rationalized by the geometry of the complexes. Even with the presence of the intracation Au–Au bonds, the linear two-coordinate geometry of gold leaves considerable space for the phosphine ligand. The largest phosphine, P(*o*-tol)$_3$, with a cone angle of 195°, shows only small distortions in the structure of the cation. Although dimerization of the $(LAu)_3O^+$ cation is observed with the smaller phosphines, the intercation bonds are not required for stability of the complexes; i.e., they do not contribute significantly to the energy of the complex. This is consistent with estimated Au(I)–Au(I) bond energies of 20–60 kJ/mol[9b,10] and our inability to detect the dimer in solution (^{31}P NMR; see above).

The wide pK_a range of the phosphine ligand is more surprising. There seems to be little effect on the structures from the pK_a variations. The average Au–O bond distances do not change over the pK_a range (2 units) examined, although there is variation (2.02–2.08 Å) in the individual distances. Insensitivity of the Au–Cl bond length of LAuCl complexes to changes in the phosphine, L, has been noted previously by Jones.[9a] In contrast, the ^{17}O NMR data do show significant changes with pK_a. While ^{17}O NMR chemical shifts are subject to a number of influences,[11] the observed linear pK_a correlation suggests electron density transfer from the phosphine ligand to the oxo group. Similarly, the ^{31}P NMR shift to lower field on going from LAuCl to the oxo complexes suggests that the oxo group's electron-withdrawing influence is felt by the phosphine ligand. What these data indicates about the nature of the Au–O interaction is not clear.

Mechanistic questions arise from the results of the oxo/chloride (eq 3) and imido/chloride exchange reactions and from the equilibration study of the imido complexes. How do these exchange processes occur? Perhaps the simplest pathway would involve the dissociation of L from the gold centers. This seems unlikely, given the high reactivity of the oxo complexes with free phosphine[12] and the high stability of the LAu fragment, which remains intact through many chemical transformations.[13] In addition, the slower exchange rates observed for the more crowded system (PPr^iPh_2) would tend to argue against a dissociative pathway. This also applies to another dissociative pathway, the dissociation of LAu^+ from **1** or **2**. In addition, previous work shows that $(LAu)_2Y$ (Y = O or NR), which would be generated from the dissociation of LAu^+ from **1** or **2**, is highly basic and rapidly and irreversibly deprotonates the solvent (CH_2Cl_2).[12] Since the exchange reactions occur in the same solvent, we do not believe that this is a likely pathway.

Dissociation of Cl^- from LAuCl to produce LAu^+ may occur. Indeed, solutions of LAu^+ are readily generated from LAuCl and Ag^+. Exchange could then occur through an $[(LAu)_4Y]^{2+}$ type intermediate (Scheme I) from the association of LAu^+ with **1** or **2**. Complexes isolobal with the proposed intermediates, $[(LAu)_4N]^+$ (for Y = 0)[14] and $[(LAu)_4CR]^+$ (for Y = NR),[15] are known. This type of intermediate would explain the slower exchange rates with the imido complexes and with the bulkier phosphine (PPr^iPh_2) since these systems would be more crowded. The intermediacy of LAu^+ is not essential for the oxo/Cl and imido/Cl exchange. A concerted reaction with a four-centered transition state, as depicted in Scheme II, would avoid Cl^- dissociation. A similar concerted process is needed to explain the imido/imido exchange reactions (Scheme III) and could also be operative in oxo/oxo exchange.

Scheme II

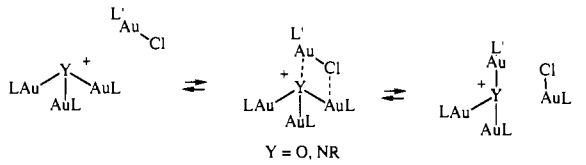

Scheme III

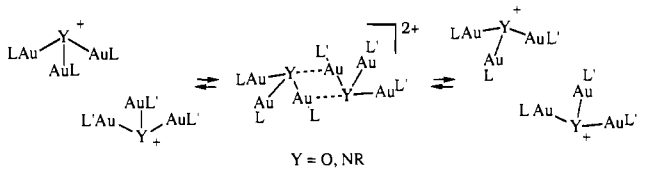

Conclusions

A large range of gold oxo complexes of the form $[(LAu)_3(\mu_3\text{-}O)]^+$ can be prepared, allowing the investigation of phosphine basicity and size in reactions where the oxo complexes are used as starting materials. In the solid state, the cation–cation interactions which lead to dimerization of the cation are subject to steric strain and can be completely disrupted with a sufficiently large phosphine. The internal structure of the cation, however, is relatively insensitive to the phosphine. In solution, rapid exchange processes between oxo and chloro complexes and imido complexes occur, leading to equilibrium mixtures. The exchange processes appear to slow with increasing steric pressure, suggesting associative pathways.

Experimental Section

General Procedures. Experiments involving air-sensitive phosphines were performed under a dinitrogen atmosphere in a VAC drybox or by Schlenk techniques. In general, once the phosphines were coordinated to the Au center, experiments were conducted in air. Reagent grade solvents were used without purification except for the synthesis of the ^{17}O-labeled complexes (see below) in which case they were carefully dried and kept under N_2. LAuCl complexes were prepared by literature techniques (L = PPh_2Me, $P(OMe)_3$)[16] or by the procedures described below. Phosphines and sulfides were used as received (Aldrich or Strem). NMR shifts are reported in ppm referenced to TMS for ^{1}H, to external H_3PO_4 (85%) for ^{31}P, and to external H_2O for ^{17}O. Microanalyses were performed by Oneida Research Services, Inc.

$[(LAu)_3O](BF_4)$ (1). The gold oxo complexes were prepared by slight modifications of procedures for the PPh_3 complex. Representative examples are given below with data for the complexes given in Table I. Yields are 80–90%.

Method A. L = $PMePh_2$, PMe_2Ph, $PEtPh_2$, P(*o*-tol)$_3$, $P(OPh)Ph_2$, $P(OEt)Ph_2$, and $P(OMe)_3$. Silver nitrate (0.8 g, 4.7 mmol) was dissolved in distilled water, and a NaOH solution was added until the pH of the mixture was between 7 and 14. The resulting brown-black precipitate of Ag_2O was allowed to settle. The supernatant was decanted, and the solid was washed successively with water, ethanol, and acetone and dried in vacuo. The freshly prepared Ag_2O was added along with 0.8 g of $NaBF_4$ (7.28 mmol) to a solution of LAuCl (1.3 mmol) in acetone (100 mL). After vigorous stirring for 1 h, the acetone was removed under reduced pressure and the residue was extracted with CH_2Cl_2 (3 × 7 mL). The combined CH_2Cl_2 extracts were filtered, and ether (3 vols) was added. In most cases, a white precipitate of the product formed, which was filtered off, washed with ether, and dried in vacuo. In two cases (L = $PMePh_2$ and PMe_2Ph), an oil was produced, which was triturated with ether until a pale brown solid was obtained. The crude product gives

(10) Schmidbaur, H.; Graf, W.; Müller, G. *Angew. Chem., Int. Ed. Engl.* **1988**, *27*, 417. (b) Jansen, M. *Angew. Chem., Int. Ed. Engl.* **1987**, *26*, 1098.
(11) *^{17}O NMR Spectroscopy in Organic Chemistry*; Boykin, D. W., Ed.; CRC Press, Inc.: Boca Raton, FL, 1991.
(12) Ramamoorthy, V. Unpublished results.
(13) Puddephatt, R. J. *The Chemistry of Gold*; Elsevier: Amsterdam, 1978. Puddephatt, R. J. In *Comprehensive Coordination Chemistry*; Wilkinson, G.; Gillard, R. D.; McLeverty, J. A., Eds.; Pergamon: Oxford, U.K., 1985; Vol. 2.
(14) Slovokhotov, Y. L.; Struchkov, Y. T. *J. Organomet. Chem.* **1984**, *277*, 143–146.
(15) Scherbaum, F.; Huber, B.; Müller, G.; Schmidbaur, H. *Angew. Chem., Int. Ed. Engl.* **1988**, *27*, 1542–1544.
(16) Williamson, D. R.; Baird, M. C. *J. Inorg. Nucl. Chem.* **1972**, *34*, 3393.

good NMR spectra and may be used in other reactions. Recrystallization is achieved by dissolving the solid in a minimum volume of CH_2Cl_2, adding an equal volume of ether, and cooling the mixture at −20 °C for 1–3 days.

Method B. From $AgBF_4$ and NaOH (L = P(*p*-ClPh)$_3$). A solution of $AgBF_4$ (33.6 mg, 0.173 mmol) in methanol (1 mL) was added to P(*p*-ClPh)$_3$AuCl (101.2 mg, 0.169 mmol) in THF (3 mL). The resulting AgCl precipitate was filtered off. A solution of KOH (10.8 mg, 0.299 mmol) and $NaBF_4$ (84.0 mg, 0.765 mmol) in methanol (20 mL) was added to the filtrate. After 1 h of stirring, the solvent was removed in vacuo. The resulting residue was extracted with CH_2Cl_2 (3 × 20 mL). The combined CH_2Cl_2 extracts were filtered, and ether (large excess) was added to precipitate the white product.

[(LAu)$_3$(μ_3-^{17}O]BF_4. The procedure is similar to that used in method B above except that all procedures were conducted under N_2, the solvents were carefully dried (MeOH was distilled from Mg turnings and THF was distilled from Na/benzophenone), and $H_2{}^{17}O$ (30%) was added to the KOH/$NaBF_4$ methanol solution. A representative example is given below.

L = PPh_3. A solution of $AgBF_4$ (0.04 g, 2.05 mmol) in methanol (10 mL) was added to a stirred THF (40 mL) solution of $AuPPh_3Cl$ (1.0 g, 2.0 mmol). After 30 min, the AgCl precipitate was removed by filtration. A mixture of 50 μL of $H_2{}^{17}O$, KOH (0.20 g, 3.6 mmol), and $NaBF_4$ (1.0 g, 4.6 mmol) in dry methanol (15 mL) was added dropwise to the stirred filtrate. After 1 h, the volatiles were removed in vacuo and the residue was extracted with CH_2Cl_2 (3 × 15 mL). Hexane (150 mL) was added to the extract. The resulting white precipitate was isolated and dried in vacuo (0.80 g, 80% yield).

LAuCl. L = $PPhMe_2$.[17] $HAuCl_4{\cdot}3H_2O$ (0.914 g, 2.32 mmol) was dissolved in ethanol (13 mL), and the solution was cooled to 0 °C and treated with thiodiglycol (0.850 g, 6.96 mmol) in ethanol under N_2. As soon as the initial yellow color had vanished, $PPhMe_2$ (0.321 g, 2.32 mmol) in 13 mL of acetone was added. The solution was stirred for 1 h and then concentrated slowly to yield 0.649 g (78%) of white product. Mp: 131–133 °C (lit.[16] 132–134 °C). $^{31}P\{^1H\}$ NMR (36 MHz, CH_2Cl_2): 4.6 ppm. ^1H NMR (300 MHz, $CDCl_3$): 1.86 ppm (d, J_{PH} = 10.8 Hz) and phenyl resonances.

L = PPh_2Et. Neat PPh_2Et (0.281 g, 1.313 mmol) was slowly added to a stirred aqueous solution of $HAuCl_4{\cdot}3H_2O$ (0.246 g, 0.625 mmol) at 0 °C. An immediate yellow precipitate was observed which became white after stirring for 1 h. The white precipitate was filtered off, washed with water, and dried in vacuo. Yield: 0.220 g (79%). $^{31}P\{^1H\}$ NMR (36 MHz, CH_2Cl_2): 33.0 ppm. ^1H NMR (300 MHz, CD_2Cl_2): 2.71 (dq, J_{HH} = 8, J_{HP} = 10 Hz), 1.29 ppm (dt, J_{PH} = 20 Hz), and phenyl resonances.

L = $PPh_2(OEt)$. $PPh_2(OPh)$ (0.505 g, 1.81 mmol) dissolved in 2 mL of ethanol was added to $HAuCl_4$ (0.865 mmol, 0.173 M in water) in ethanol (10 mL) at 0 °C under N_2. A yellow precipitate was observed at once. After vigorous stirring for 1 h, the mixture was warmed to room temperature. The resulting white precipitate was isolated by filtration, washed with ethanol, and dried in vacuo. Yield: 0.240 g (60%). The spectroscopic data for the product and for the oxo complex derived from it showed that exchange of the phosphite OPh group with ethanol had occurred. $^{31}P\{^1H\}$ NMR (36 MHz, CH_2Cl_2): 109.0 ppm. ^1H NMR (300 MHz, $CDCl_3$): 4.20 (dq, J_{HH} = 7.0, J_{HP} = 9.7 Hz), 1.43 ppm (t), and phenyl resonances.

L = $PPh_2(OPh)$. Me_2SAuCl (211.6 mg, 0.718 mmol) in CH_2Cl_2 (2 mL) was added with stirring to $PPh_2(OPh)$ (200 mg, 0.719 mmol) in 1 mL of CH_2Cl_2. After 10 min, the volatiles were removed in vacuo to give the white crystalline product. Yield: 0.346 g (94%). $^{31}P\{^1H\}$ NMR (36 MHz, CH_2Cl_2): 114.0 ppm.

L = $PPr^i Ph_2$. The same procedure as for $PPhMe_2$ was used. Yield: 95%. $^{31}P\{^1H\}$ NMR (36 MHz, CH_2Cl_2): 48.2 ppm. ^1H NMR (300 MHz, $CDCl_3$): 2.83 (dsept, J_{HH} = 6.8 Hz, J_{HP} = 18.9 Hz), 1.23 ppm (dd, J_{PH} = 19.7 Hz), and phenyl resonances.

L = (*p*-ClPh)$_3$P. The same procedure as for $PPhMe_2$ was used. Yield: 85%. $^{31}P\{^1H\}$ NMR (36 MHz, CH_2Cl_2): 32.0 ppm.

L = P(*o*-tol)$_3$. The same procedure as for $PPhMe_2$ was used. Yield: 86%. $^{31}P\{^1H\}$ NMR (36 MHz, CH_2Cl_2): 8.48 ppm. ^1H NMR (300 MHz, $CDCl_3$): 2.68 ppm (s).

L = $P(OMe)_3$. The procedure used is described in ref 16. Mp: 96–97 °C (lit.[16] 100–101 °C). $^{31}P\{^1H\}$ NMR (36 MHz, CH_2Cl_2): 121.1 ppm. ^1H NMR (300 MHz, $CDCl_3$): 3.80 ppm (d, J_{HP} = 14.0 Hz).

L = PPh_2Me. The procedure used is described in ref 16. $^{31}P\{^1H\}$ NMR (36 MHz, CH_2Cl_2): 17.2 ppm. ^1H NMR (300 MHz, $CDCl_3$): 2.15 ppm (d, J_{HP} = 10.4 Hz) and phenyl resonances.

Structure Analyses. Crystals were selected while submerged in oil, transferred to 5-min epoxy that had been allowed to set for several minutes, and then mounted, with a coating of epoxy, on the end of a glass fiber. This technique prevents loss of the solvent of crystallization, which was a problem for all of the samples studied. Data collection (CAD4) and reduction and the structure solution (direct methods) and refinements followed standard procedures. A summary outline of crystallographic and data collection parameters is given in Table II. Details of the data collection and reduction and the structure solution and refinement are provided as supplementary material.

Acknowledgment. We thank the Division of Chemical Sciences, Office of Basic Energy Sciences, Office of Energy Research, U.S. Department of Energy (Grant DE-FG02-88ER13880), for support of this work. Grants from the National Science Foundation provided a portion of the funds for the purchase of the X-ray (CHE-9011804) and NMR (PCM-8115599 and CHE 89-08304) equipment.

Supplementary Material Available: A plot of the ^{17}O NMR data and listings of detailed experimental data, positional parameters, thermal parameters, and bond distances and angles (25 pages). Ordering information is given on any current masthead page.

(17) Adapted from: Al-Sa'Ady, A. K.; McAuliffe, C. A.; Parish, R. V.; Sandbark, J. A. *Inorg. Synth.* **1985**, *23*, 191 (as referenced in: Steigelmann, O.; Bissinger, P.; Schmidbaur, H. *Angew. Chem., Int. Ed. Engl.* **1990**, *29*, 1399–1400).